

## FATIGUE CRACK GROWTH BEHAVIOUR OF THE FRICTION STIR WELDED 6082-T6 ALUMINIUM ALLOY

Moreira, P.M.G.P.<sup>1</sup>; Jesus, A.M.P.<sup>2</sup>; Ribeiro, A.S.<sup>3</sup>; Castro, P.M.S.T.<sup>4</sup>

<sup>1</sup>Bolseiro de Investigação, <sup>4</sup>Prof. Catedrático

DEMEGI, Faculdade de Engenharia da Universidade do Porto

<sup>3</sup>Prof. Auxiliar, <sup>4</sup>Prof. Associado c/ Agregação

Departamento de Engenharias, Universidade de Trás-os-Montes e Alto Douro



### RESUMO

*A study on fatigue crack growth behaviour of friction stir butt welds of 3mm thick 6082-T6 aluminium alloy was performed. Fatigue crack growth curves were determined for cracks growing in different locations of the weldments, namely the base material, friction stirred material and heat affected material. Results are complemented with monotonic tensile data, microhardness measurements and scanning electron microscopy observations. Friction stir material exhibited lower tensile strength and ductility properties than base material. However, an enhanced crack propagation resistance is observed.*

### 1- INTRODUCTION

The increasing relevance of aluminium alloys in transportation requires research on more efficient and reliable joining processes. Friction stir welding (FSW) is a solid-state joining process, which emerged as an alternative technology to be used in high strength alloys that were difficult to join with conventional techniques. The process was developed initially for aluminium alloys, but since then FSW was found suitable for joining a large number of materials. In FSW the interaction of a non consumable and rotating tool with the workpieces being welded creates a welded joint through frictional heating and plastic deformation at temperatures below the melting temperature of the alloys being joined. Notwithstanding the widespread interest in the possibilities offered by FSW, data concerning the mechanical behaviour

of joints obtained using this process is still scarce. Research work on fatigue crack growth data from the weld zone is required to provide tools to assess the damage tolerance issues. In this work a study on fatigue crack growth behaviour of friction stir (FS) butt welds of a 3mm thick age hardenable 6082-T6 aluminium alloy was carried out. Fatigue crack growth curves were determined for cracks growing in different locations of the weldments, including the base material (BM), the heat affected zone (HAZ) and the welded material (WM). This study also included monotonic tensile tests of base material and welded joints in order to understand the influence of the welding process on the static strength. Microhardness profiles were measured and Scanning Electron Microscopy (SEM) observations carried out on the fracture surfaces.

## 2–MATERIAL AND WELDING PROCESS

The 6082-T6 aluminium alloy is a high strength Al–Mg–Si alloy that contains manganese to increase ductility and toughness. The T6 condition is obtained through artificial ageing at a temperature of approximately 180°C [Ericsson and Sandstrom (2003)]. The friction stir welds were performed using the following parameters: welding speed of 800mm/min; pitch angle of 2°; rotating speed of 1500rpm. A tool with a 6mm diameter threaded pin and shoulder with 15mm diameter was used.

## 3–MONOTONIC TENSILE TESTS

Monotonic tensile tests were performed to determine the mechanical properties of the welded and unwelded materials: the yield stress  $\sigma_y$ , the rupture stress  $\sigma_r$ , the Young modulus E, and the elongation at failure  $\epsilon_r$ . The tests were performed using standard rectangular tension test specimens [ASTM E08-04 (2004)]. Table 1 summarizes average values of those properties, extracted from the monotonic tensile curves. The table also includes reference values from the base materials supplier. The monotonic tensile tests revealed higher strength and ductility properties than values given by the supplier data. All base material specimens failed in the same manner, according to 45° shear planes. In the friction stir welded specimens, fracture occurred near the weld edge line. This failure location is characterised by the lowest hardness as demonstrated by figure 1 and documented in [Scialpi et al. (2007)]. It was also verified that the fracture occurred according to 45° shear planes. This type of fracture surface is also documented by [Svensson et al. (2000)] when testing the same alloy. The elongation of all friction stir welded specimens is approximately 32% of the base material; they present a yield stress of 51% of the base material. Concerning the stress at rupture the result is more encouraging since the friction stir welded specimens exhibited a stress at rupture about 70% of the base material. Scialpi et

al. (2007) using 1.5mm thick friction stir welded Al6082-T6 specimens obtained a stress at rupture of about 76% of the base material; this values is of the same magnitude of the one obtained in this study. Ericsson et al. (2003) when welding 4mm butt joints of Al6082-T6 alloy found values for the yield and rupture stresses of the same magnitude of this study. Also, values of the same magnitude are reported by Harris and Norman (2003) and Nicholas and Kalle (2000) in their literature review about the FSW process. Dickerson and Przydatek (2003) obtained lower values of yield and rupture stresses using FSW 6mm thick plates of Al6082-T6.

**Table 1** – Monotonic properties for base material and FS welded specimens.

Material type	$\sigma_y$ [MPa]	$\sigma_r$ [MPa]	E [GPa]	$\epsilon_r$ [%]
6082-T6 supplier certificate	>260	310	69	10
6082-T6	276.2	322.9	67.1	17.5
FSW	140.5	226.1	49.4	5.5

## 4–MICROHARDNESS MEASUREMENTS

The hardness profiles can assist the interpretation of the weld microstructures and mechanical properties. Microhardness tests were performed in order to characterize the hardness profile in the vicinity of the weld affected area. The microhardness tests were performed across the weld zone and into the parent material using a 100gf load. The microhardness tests were performed at the specimens' middle thickness. Figure 1 illustrates the Vickers hardness profile. A hardness decrease is verified in the thermo-mechanically affected zone (TMAZ). The average hardness of the nugget zone (NZ) was found to be significantly lower than the hardness of the base alloy. There is a zone outside the nugget zone which has the lower hardness value, and the hardness increases in the HAZ towards the parent material. The welding process softened the material reducing the hardness to 33% of the parent material, as shown by Scialpi et al. (2007). Harris et al. (2003) suggested that the

variation of the microhardness values in the welded area and parent material is due to the difference between the microstructures of the base alloy and weld zone.

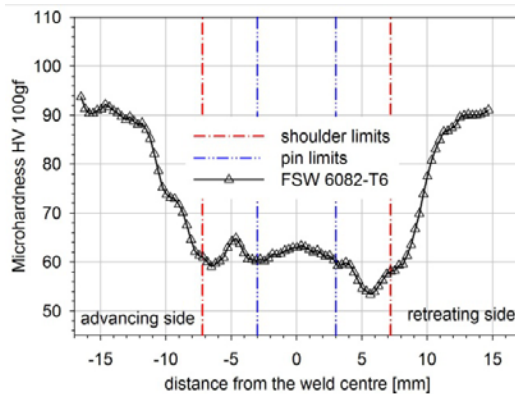


**Fig 1** - Microhardness profile of the FS welded 6082-T6 aluminum alloy.

## 5–FATIGUE CRACK GROWTH DATA

Since currently a very limited amount of data on fatigue crack growth in FS welded joints is available in the literature, this manuscript presents a study on fatigue crack growth data of FS butt welds made of 3mm thick age hardenable 6082-T6 aluminium alloy. Both BM, HAZ and FS welded materials are investigated. All fatigue experiments were carried out under constant load amplitude, at room temperature and in laboratory air on a computer controlled servo-hydraulic INSTRON 801 testing machine, following the ASTM E647 standard. Crack propagation was monitored through visual measurements using a travelling microscope. “As-welded” 40mm wide compact tension (CT) specimens were tested for a 20Hz load frequency. Figure 2 illustrates the tested crack paths orientation, in relation to the weld location.

Figure 3 summarizes the main results obtained for the BM tested under  $R=0.1$  and  $R=0.5$ . Figure 4 presents results of the FS welded specimens. It is verified that for lower/intermediate stress intensity factor ranges ( $\Delta K$ ), the crack propagation rates of the base material in the rolling and transverse directions are very close; for higher  $\Delta K$  some deviation are encountered – the crack growth rates in the rolling direction are greater than in transverse direction. It is interesting to note

that the friction stir material has markedly lower crack propagation rates than the HAZ and the base material. One possible explanation can be the residual stress distribution in the crack vicinity. Figure 5 illustrates the typical stress distribution expected in friction stir plates and at crack vicinity of CT specimens. It is verified that compressive stresses appears at crack vicinity which can result in a crack growth retardation effect [Ghidini e Donne (2006), Biallas et al. (2006)]. The graphs from figures 4 and 5 also include the Paris’s law correlation which is achieved for very high correlation coefficients.

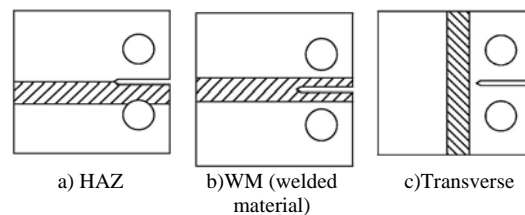


**Fig 2**- Tested crack path orientations.

Table 2 compares the constants of the Paris’s law obtained in this study, with the constants from other sources, such as Borrego et al. (2001), Eurocode 9 (1998) and T. Mann (2006). Constants proposed by Borrego et al (2001) were derived with middle tension specimens with a thickness of 3mm for cracks propagating in the L-T system. The crack propagation was measured using optical devices. T. Mann (2006) tested single edge notch tension (SENT) specimens with thicknesses in the range 2.8-3.2mm, extracted from RHS profiles. This author used the DC potential drop technique to measure the crack growth. Each entry in the table from the latter author corresponds to values from single tests. Figure 6 compares the crack propagation rates for  $R=0.1$ . It can be seen a good agreement between the data from the current study and Borrego et al. (2001) and the Eurocode 9. The Eurocode 9 proposes the higher crack propagation values, which is consistent with the fact that the Eurocode 9 incorporates safety margins. The three crack propagation curves from T. Mann (2006) show significant scatter. However, an average crack propagation curve would likely fit within the range of the other sources.

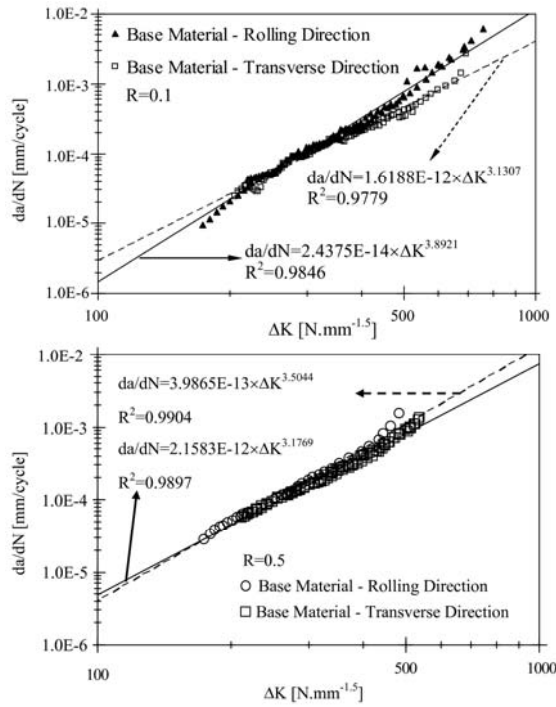


Fig 3 – Fatigue crack propagation data for the 6082-T6 base material.

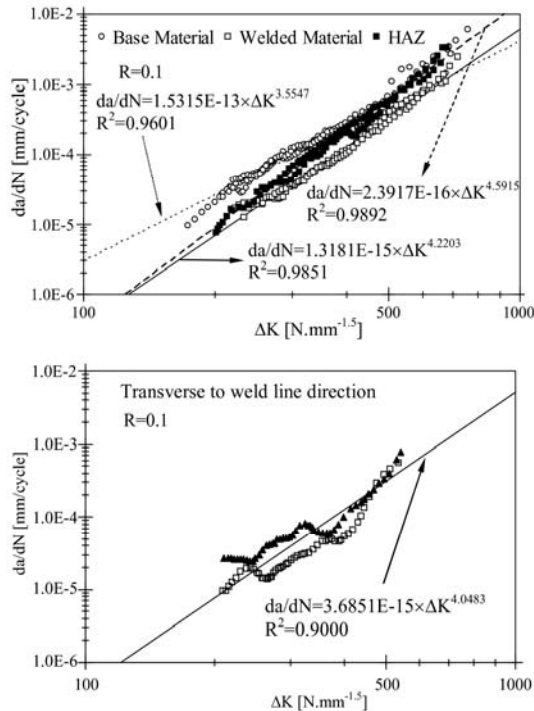


Fig 4 – Fatigue crack propagation data for 6082-T6 FS welded specimens.

## 6-SEMANALYSIS OF CT SPECIMENS

Three different friction stir welded AA6082-T6 compact tension specimens were analysed using SEM. Three crack configurations were investigated: crack in the HAZ, crack at the middle of the weldment and

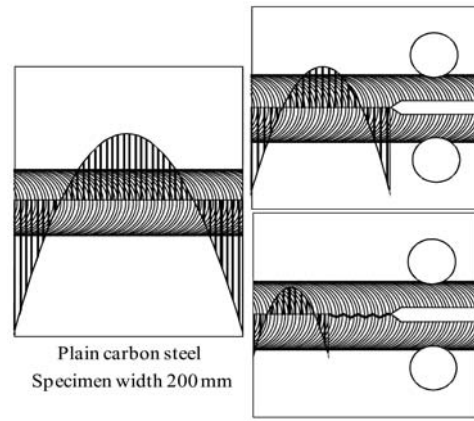


Fig 5 – Typical residual stress distributions on welded specimens [Ohta et al. (1982)].

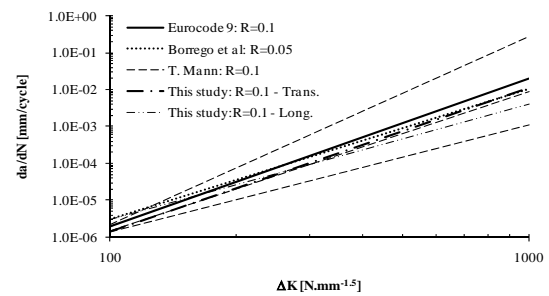


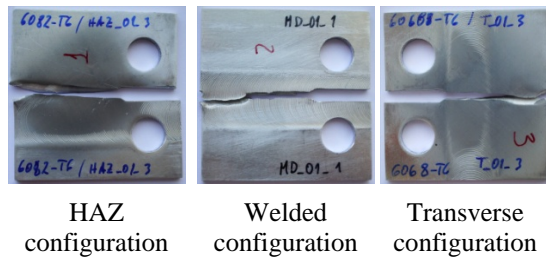
Fig 6 – Comparison between crack propagation rates according several sources for the AA6082-T6.

Table 2 – Constants of the Paris law for the AA6082-T6 according to several sources.

Source	R-Ratio	C mm/cycle; $N \cdot mm^{-1.5}$	m	$R^2$
This study	0.00 – Long.	4.4E-14	3.73	0.972
	0.10 – Long.	2.4E-14	3.89	0.985
	0.10 – Trans.	1.6E-12	3.13	0.978
	0.50 – Long.	4.0E-13	3.50	0.990
	0.50 – Trans.	2.2E-12	3.18	0.990
Borrego et al. (2001) (L-T propagation system)	0.40	9.5E-13	3.40	0.996
	0.25	5.9E-13	3.45	0.998
	0.05	2.5E-13	3.54	0.998
	-0.25	2.0E-14	3.98	0.998
Eurocode 9 (1998)	0.10	2.0E-14	4.00	-
	0.50	1.1E-13	3.90	-
T. Mann (2006)	0.10	1.4E-16	5.10	-
	0.10	2.2E-12	2.90	-
	0.10	3.6E-14	3.80	-
	0.30	1.6E-14	4.20	-
	0.50	1.1E-11	2.90	-
	0.50	4.4E-12	3.00	-
	0.80	2.0E-12	3.40	-

crack transverse to the weldment, as illustrated in figure 7. For all specimens configuration, measurable fatigue striations were difficult to identify. The macrographs of the different

crack surfaces that were found in each specimen are presented in figure 8.



**Fig 7** – Fractured CT specimens analyzed using SEM.

When the crack grows in the HAZ there are no visually identifiable particular features, figure 8a), but if the crack grows at the middle of the weld bead striations related with the tool advance per revolution are a characteristic of the surface, figure 8b). For a crack growing transverse to the weldment, different zones are identified, figure 8c). First a regular surface corresponding to the HAZ is present, but when the crack reaches the TMAZ, layers of stirred material, frequently called as onion rings, as marked on the surface, are visible.

### 6.1 - CT specimen with a crack propagating in the HAZ

The first specimen analyzed with SEM has a crack that propagated in the HAZ. Details of the crack surface are presented in figure 9. It was verified that the crack surface becomes rougher for higher crack lengths. Figures 9e) and 9f) show higher magnification fractographs of particular

details, as faded fatigue striations and voids.

### 6.2 - CT specimen with a crack propagating at the middle of the weldment

The second specimen analyzed has a crack that grew at the middle of the weldment. The fatigue crack surface was similar along all its length, presenting striations which correspond to the tool advancing per revolution, as already presented in the figure 8b) (macrograph). The fatigue crack surface near the initial notch and a detail of its heterogeneous structure is presented in figures 10a) and 10b). The striations, which correspond to the tool advance per revolution, are presented in figures 10c) and 10d). The crack surface is found to be different in the two different zones of each striation mark, as presented in figure 10e) and 10f).

### 6.3 - CT specimen with a crack propagating transverse to the weld bead

The last specimen analyzed has a crack that grew transversely to the weldment, crossing the HAZ and then the TMAZ. In the HAZ the crack surface, as presented in figure 11, is similar to the one found in the first specimen analyzed. The zone where the fatigue crack crossed the stirred material zone, TMAZ, has a topography which corresponds to the material flow during the friction stir welding process, figure 12. The layers of material flow at the weld nugget can now be easily identified.

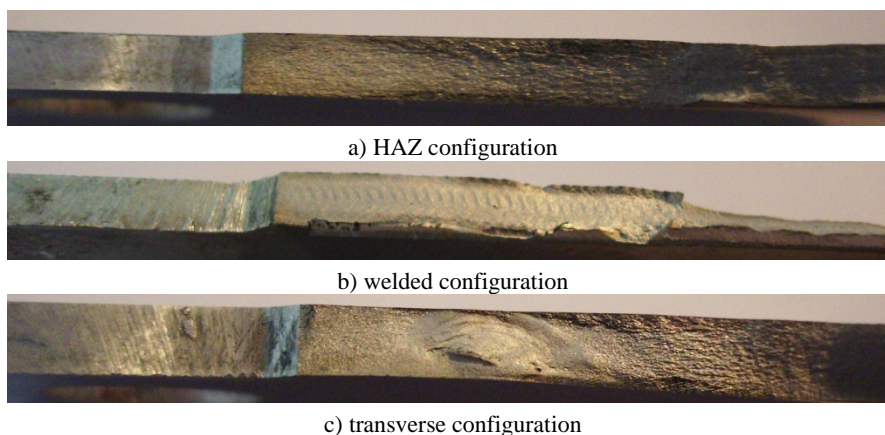


**Fig 8** – Fracture surface of different CT specimens (macrographs).



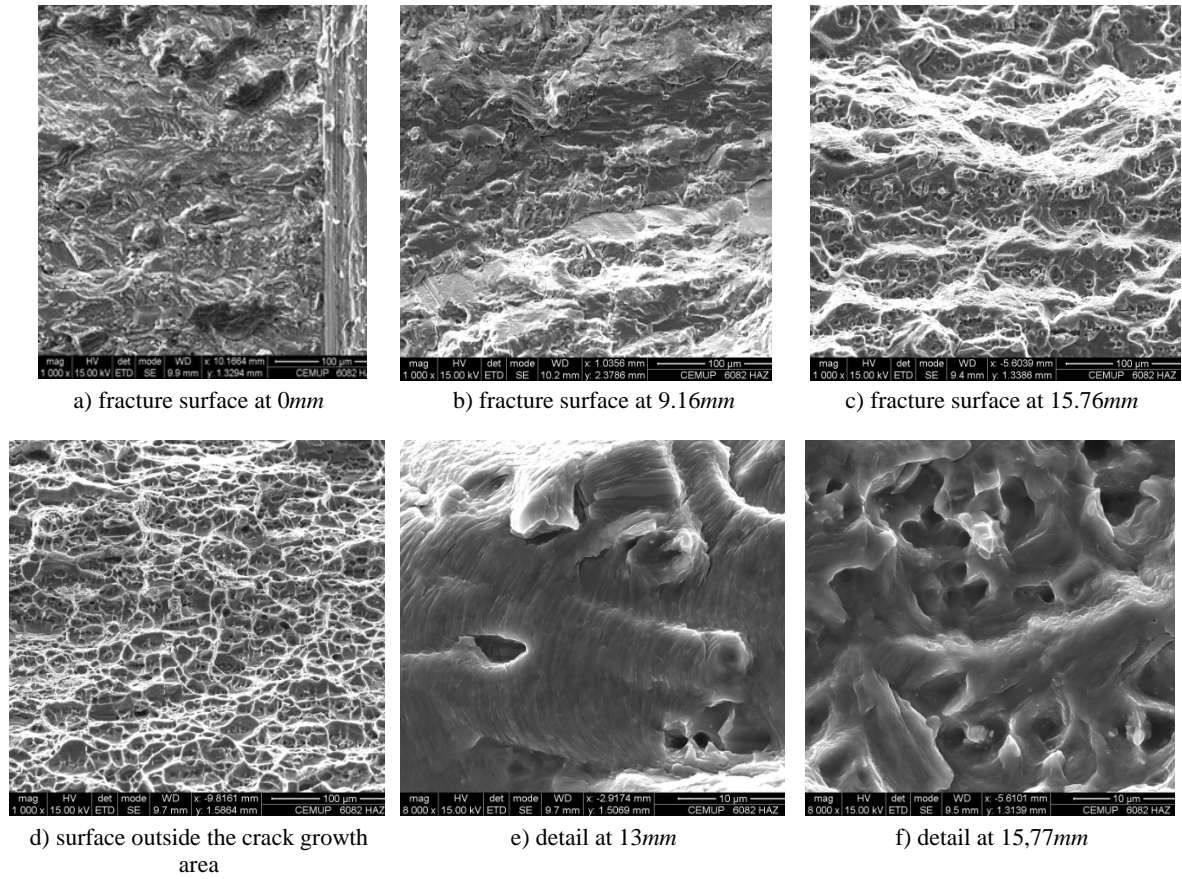


**Fig 9** - Fracture surface for different crack lengths propagating in the HAZ.

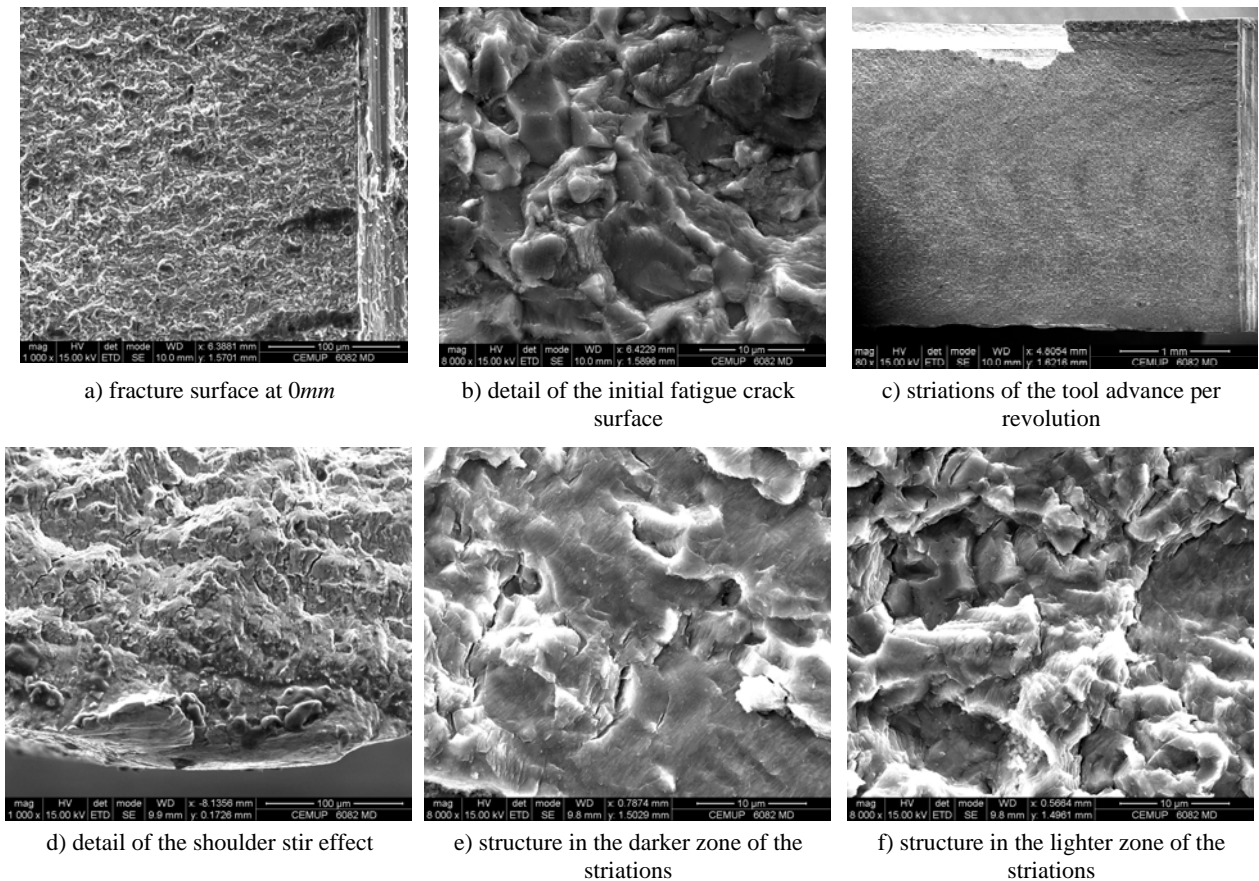


**Fig 10** - Fracture surface for different crack lengths propagating in the middle of the weldment.

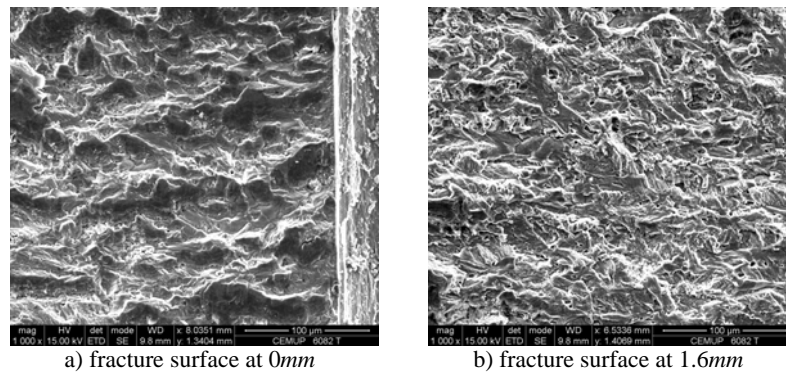


**Fig 11** - Fracture surface details for different crack lengths propagating transversely to weld bead.

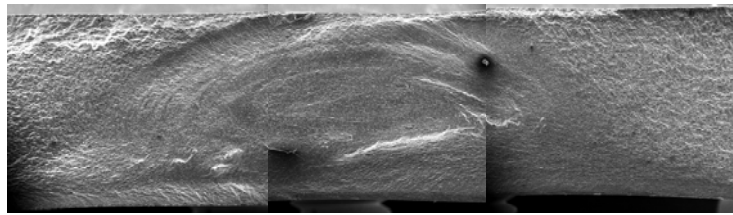


**Fig 12** - Fracture surface at the weld nugget

## 7 – CONCLUSIONS

Friction stir butt welds of 6082-T6 aluminium alloy plates were investigated. The friction stir welded material revealed lower yield and ultimate stresses than the base material as well as lower elongation and hardness. For the monotonic tensile tests, failures occurred near the weld edge line. The fatigue crack growth behaviour was characterized for different material locations from the friction stir weld, namely the base material, HAZ and friction stir material. An increase of the crack propagation resistance, i.e. lower crack propagation rates, was verified for the welded material in comparison with the HAZ or even the base material, which is consistent with a compressive residual stress field at the crack vicinity. SEM observations were performed for the three types of crack propagation paths illustrating the typical microstructures.

## ACKNOWLEDGMENTS

The work was partially supported by contracts FCT SFRH/BD/19281/2004 and PTDC/EME-TME/66362/2006, and UE

contract no. AST3-CT-2004–516053. The laboratorial work of Rui Silva (FEUP), Daniela Silva (CEMUP) and the collaboration of Rui Louro (ISQ) are also gratefully acknowledged.

## REFERENCES

- Ericsson, M., Sandstrom, R., Influence of welding speed on the fatigue of friction stir welds, and comparison with MIG and TIG, International Journal of Fatigue, Vol. 25, pp. 1379–1387, 2003.
- ASTM E8–04, Standard Test Methods for Tension Testing of Metallic Materials. 2004.
- Scialpi, A., De Filippis, L.A.C., Cavaliere, P., Influence of shoulder geometry on microstructure and mechanical properties of friction stir welded 6082 aluminium alloy, Materials and Design, Vol. 28 (4), pp. 1124–1129, 2007.
- Svensson, L.E., Karlsson, L., Larsson, H., Karlsson, B., Fazzini, M. and Karlsson, J., Microstructure and mechanical properties of friction stir welded aluminium alloys with special reference to AA 5083 and AA 6082, Science and Technology of Welding & Joining, Vol. 5 (5), pp. 285–296, 2000.
- Harris, D., Norman, A.F., Properties of Friction Stir Welded Joints: A Review of the

- Literature, Progress report presented at the 6th PSG Meeting, 17-18 June 2003.
- Borrego L. P., Ferreira J. M. and Costa J. M., Fatigue crack growth and crack closure in an AlMgSi alloy, *Fatigue Fract. Engng Mater. Struct.* 24, p. 255–265.
- CEN. ENV 1999-2: Eurocode 9: Design of aluminium structures – Part 2: Structures susceptible to fatigue. European Committee for Standardisation; 1998.
- Mann T., Fatigue assessment methods for welded structures and their application to an aluminium T-joint, PhD Thesis, Norwegian University of Science and Technology, 2006.
- Nicholas, E.D., Kallee, S.W., Friction Stir Welding - A Decade On, IIW Asian Pacific International Congress, Sydney, 29 October - 2 November 2000.
- Dickerson, T.L., Przydatek, J., Fatigue of friction stir welds in aluminium alloys that contain root flaws, *International Journal of Fatigue*, Vol. 25, pp. 1399–1409, 2003.
- Ghidine, T., Donne, C.D., Fatigue crack propagation assessment based on residual stresses obtained through cut-compliance technique, *Fatigue Fract Engng Mater Struct*, Vol.30 (3), pp.214-222, 2007.
- Biallas, G., Alléhaux, D., Marie, F., Role of residual stresses on Fatigue Crack Propagation of FSW 6056-T78 aluminium joints under various technologies, *Materials Science Forum Vols.* 519-521, pp. 1089-1094, 2006.
- A. Ohta, E. Sasaki, M. Nihei, M. Kosuge, and M. Inagaki: Fatigue crack propagation rates and threshold stress intensity factors for welded joints of HT80 steel at several stress ratios. *International Journal of Fatigue*, vol. 4(4), pp. 233-237, 1982.